ELSEVIER

Contents lists available at ScienceDirect

NDT and E International

journal homepage: www.elsevier.com/locate/ndteint



Surface reconstruction accuracy using ultrasonic arrays: Application to non-destructive testing



Robert E. Malkin^{a,*}, Amanda C. Franklin^a, Rhodri L.T. Bevan^a, Hiroshige Kikura^b, Bruce W. Drinkwater^b

- a Department of Mechanical Engineering, University of Bristol, Bristol, UK
- ^b BS8 1TR 2 Laboratory for Advanced Nuclear Energy, Tokyo Institute of Technology, Tokyo, Japan

ABSTRACT

The accurate non-destructive inspection of engineering structures using ultrasonic immersion imaging requires a precise representation of the surface of the structure. Here we investigate the relationship between surface geometry, surface measurement error using ultrasonic arrays and the total focusing method (TFM) and how this impacts on the ability to image a feature within a component. Surfaces shaped as sinusoids covering combinations of surface wavelengths (0.8 to $32\lambda_{water}$) and amplitudes (0.6 to $9\lambda_{water}$) are studied. The surface reconstruction errors are shown to cause errors in imaging, such as reduced amplitude and blurring of the image of a side-drilled hole. These reconstruction errors are shown to increase rapidly with the maximum gradient of the sinusoid. Sinusoidal surfaces with maximum gradients $< 45^{\circ}$ lead to average surface reconstruction errors $<\lambda_{water}$ and amplitude imaging errors within 6 dB of the flat-surface case. It is also shown that very poor results are obtained if the surface gradient is excessively steep.

1. Introduction

In ultrasonic non-destructive testing (NDT) an individual transducer, or an array of transducers, are used to insonify the structure under inspection, allowing acoustic energy to propagate into the test structure and then the return echo signals are analysed. When the surface of the structure is uneven two approaches may be utilised; (A) the transducer surface is fitted with a wedge or 'shoe' which has a corresponding negative surface to allow for direct contact [1] or (B) the structure under inspection is placed in a water bath which acts as an acoustic couplant between the transducer and structure surface [2]. The use of shoes has the benefit of being simple to implement, it is however only suited to a single known surface profile and multiple shoes may be needed for even a simple inspection. The immersion approach has the benefit that it can be used for relatively complex surfaces (which need not always be known a priori), it is however limited to structures which may be submerged. There also exist a number of 'hybrid' methods which use a conformable coupling material, such as a water-filled bag, between the transducer and the test structure [3], or conformable/flexible arrays which may be placed in direct contact with a curved surface [4-7].

In any ultrasonic technique, the aim is to efficiently transfer acoustic energy from the transducer into the test structure. In order to correctly interpret the return echo signals to form an image of an internal defect the acoustic ray paths must be calculated. For the shoe case this is readily

done as the geometry and materials of both the shoe and the structure surface are known. For the immersion case the ray paths may either be calculated explicitly for a given surface position, for example, using a surface profilometer [6] or determined using the echo data itself [4]. For a surface which is not known *a priori* the echo data can be analysed to determine the location and shape of the structure surface and hence allow accurate imaging of internal features.

To date there is a lack of published literature exploring the influence of the surface geometry on the accuracy of surface reconstructions and internal feature imaging. The recent works of Kerr et al. investigated the accuracy of surface reconstructions of 3D metal samples (sphere, cuboid and cylinder) and a more complex human femur bone surface [8,9]. The aim of the present study is to build on such work and elucidate the relationship between an object's surface geometry and the resulting ability to accurately image within it, which is of importance for NDT inspections as a defect's size/severity may be underestimated due to errors in an accurate reconstruction of its surface. This is achieved in two parts, firstly we consider the impact of surface geometry on surface reconstruction accuracy and secondly the resultant impact on internal imaging quality.

Many components in engineering structures consist of curved regions which hamper the use of simple direct-contact inspection, examples include: train wheel axles, nozzle welds and turbine blades. Applying an imaging approach through such surfaces requires the location and

E-mail address: r.e.malkin@gmail.com (R.E. Malkin).

 $^{^{\}ast}$ Corresponding author.

geometry of the surface to be known. There are three common methods by which the surface geometry may be measured; (i) the geometry is taken from manufacturing diagrams/photographs or physically measured, (ii) the time of flight between single elements within the array and the surface [10,11], and (iii) the surface geometry can be extracted using an imaging approach such as the Total Focusing Method (TFM) [12, 13] or Synthetic Aperture Focusing Technique (SAFT) [8,9,14]. Even minor surface profile errors (less than a fraction of the acoustic wavelength) can result in significant loss of image quality through loss of coherence [15].

Here we use the TFM imaging algorithm [16] and a 1D array to perform 2D imaging. However, we note that the approaches described can equally be applied to other imaging algorithms and extended to 2D arrays and 3D imaging. The TFM algorithm uses all the possible combinations of transmit-receive elements of the array, shown in Fig. 1, a data-set set known as Full Matrix Capture (FMC). The TFM algorithm has been shown to have superior resolution compared to traditional imaging algorithms [17] which presents the best resolution for surface reconstruction. It should be noted however that other imaging algorithms (which may have lower spatial resolution) are able to resolve surface geometries with high accuracy [8,9].

For an array of p elements the FMC is generated by firing the first element of the array and recording the echo time domain signal on all p elements. This is repeated for all elements and results in p^2 time domain traces. Fig. 1 shows the schematic of the TFM algorithm applied to a material under inspection via a coupling medium. The TFM algorithm is applied post-capture to the FMC data and calculates the image intensity, I, of an arbitrary point, $P(x_2, z_2)$, as given by Eq. (1).

$$I(x,z) = \left| \sum_{T,R} h_{T,R}^{Hilb} \left(\frac{d_1}{c_1} + \frac{d_2}{c_2} + \frac{d_3}{c_2} + \frac{d_4}{c_1} \right) \right| \tag{1}$$

where: $h_{T,R}^{Hilb}$ is the Hilbert transform of the time domain signal from the transmitting element, $T(x_{tx}, z_{tx})$, to the receiving element, $R(x_{rx}, z_{rx})$, $d_{1:4}$ are the ray path distances between $T(x_{tx}, z_{tx})$ the point $P(x_2, z_2)$ and $R(x_{rx}, z_{rx})$, c_1 and c_2 are the longitudinal wave speeds in the coupling medium the material being imaged, respectively. The summation is performed over all possible transmitter-received combinations.

As the longitudinal velocity in the water and the material, c_1 and c_2 , are dissimilar the ray paths between array elements and points of interest within the structure need to be calculated. This is achieved by calculating

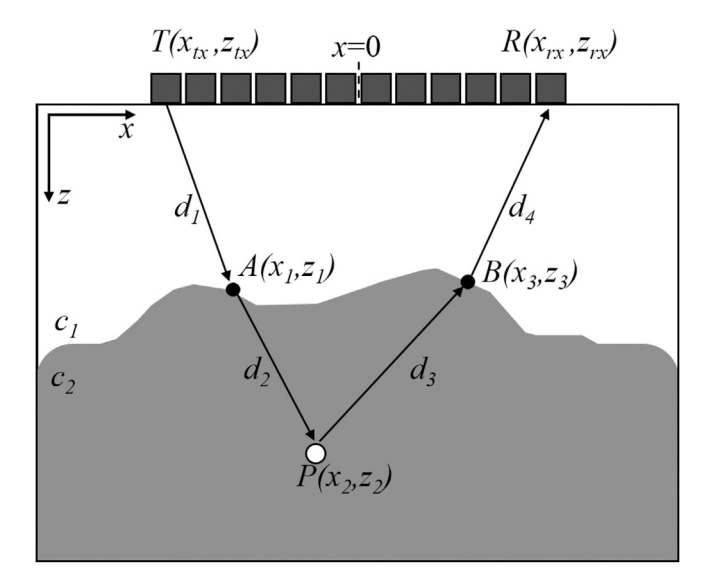


Fig. 1. Application of the TFM algorithm to a test structure in immersion. $c_1 \& c_2$ are the longitudinal wave speed speeds in the immersion fluid (usually water) and the test structure respectively.

the minimum time-of-flight from $T(x_{tx},z_{tx})$ to $A(x_1,z_1)$ to $P(x_2,z_2)$ to $B(x_3,z_3)$ to $R(x_{rx},z_{rx})$ which are the distances $d_{1:4}$ [2,12]. For this calculation the points $A(x_1,z_1)$ and $B(x_3,z_3)$ in Fig. 1 need to be found. This is achieved by applying the TFM (or other imaging algorithm) to the whole imaging area and forming a fine image of the interface between the water and the test structure. With the interface measured the minimum time-of-flight between each transmitting and receiving element via each point on the surface is calculated (using Fermat's principle of least time), which in Fig. 1 would be distances $d_{1:4}$.

2. Test specimens and experimental set-up

To directly address the impact of surface geometry we manufacture a number of sinusoidal-shaped surfaces, the rationale being that arbitrary surfaces may be decomposed into a number of sinusoidal components. As shown in Figs. 2a and 3 and Table 1, surfaces of 300mm in length were formed from n = 10 single-cycle sine waves of different wavelengths, ψ_n . Ten amplitude-scaled versions of this surface were then formed to cover a wide range of surface geometries. The amplitude and wavelength of the surfaces are given in terms of the acoustic wavelengths, λ_w , (in water for a central transducer frequency of 5MHz), in Table 1. At one extreme, this range included relatively flat surfaces where both the amplitude and feature wavelength are $<\lambda_w$. At the other extreme highly curved surfaces are included that cause significant image distortion. Each sample also included two flat 5mm sections at both ends to act as reference positions. This resulted in 100 single-cycle sine waves with unique combinations of amplitude and wavelength. To study internal imaging a 2mm diameter side-drilled hole (SDH) was introduced 10mm below each sinusoid, shown in Fig. 2b. The surfaces shown in Fig. 2 were manufactured by laser cutting 4 layers of 5mm thick acrylic (c = 2730 m/s; density, $\rho =$ $1180kg/m^3$) and bonded to create 20mm thick samples.

The maximum gradient of the surface is use to characterise its severity and is given by,

$$\sigma_{m,n} = tan^{-1} \left(\frac{2\pi Amp_m}{\psi_n} \right) \tag{2}$$

where 0° is a flat surface and 90° would be a vertical step. The value of σ for the range of amplitudes (m=1:10) and surface lengths (n=1:10) featured in the 100 manufactured surfaces is shown in Figure 3.

The samples were immersed in a 3-axis computer-controlled scanning system. To image a whole specimen (in length) the array (see table 2 for details) was moved in 10mm increments a total of 31 times. Throughout all measurements the probe was held parallel to the z axis. With a known surface geometry it is possible to orientate the array to be parallel to the surface under inspection to maximise transmission of acoustic energy into the sample. Given the array being much larger than many of the spatial features we investigated and making no surface geometry assumptions we kept the array orientation to the sample surfaces fixed. The scanning of the array location and data acquisition was fully automated. At each array location a FMC dataset was captured and a corresponding TFM image created and digitally stored, shown in Fig. 4.

When applying the TFM algorithm to extract the surface of a sample the ray paths are assumed to be direct and unobstructed. For surfaces with relatively small Amp this is generally true, however for larger values of Amp and shorter ψ , as shown diagrammatically in Fig. 5, the ray paths may be obstructed resulting in path shadowing. We approximate that spatial surface features which will result in shadowing to occur when the ratio of $\frac{\psi}{Amp} < \frac{w}{h}$, where w is the array width. Shadowing will occur for surfaces when $\frac{\psi}{Amp} < \frac{w}{h} = \frac{\psi}{Amp} < 0.56$, where h = 85mm. A ratio of 0.56 is the equivalent of the maximum surface inclination angle of $\sigma = 15.6^{\circ}$.

A TFM_{global} image was formed by image stitching; i.e. the process of combining multiple TFM_{local} images with overlapping areas to produce a single TFM_{global} image larger in size than the individual images. To summarise, we used image pixels spaced by 0.1mm in both x and z axes

Download English Version:

https://daneshyari.com/en/article/6758260

Download Persian Version:

https://daneshyari.com/article/6758260

<u>Daneshyari.com</u>